Monochromatic aberrations of the human eye in a large population

Jason Porter

The Institute of Optics, University of Rochester, Rochester, New York 14627

Antonio Guirao*

Center for Visual Science, University of Rochester, Rochester, New York 14627

Ian G. Cox

Bausch & Lomb, Rochester, New York 14692

David R. Williams

Center for Visual Science, University of Rochester, Rochester, New York 14627

Received August 21, 2000; revised manuscript received January 2, 2001; accepted February 20, 2001

From both a fundamental and a clinical point of view, it is necessary to know the distribution of the eye's aberrations in the normal population and to be able to describe them as efficiently as possible. We used a modified Hartmann–Shack wave-front sensor to measure the monochromatic wave aberration of both eyes for 109 normal human subjects across a 5.7-mm pupil. We analyzed the distribution of the eye's aberrations in the population and found that most Zernike modes are relatively uncorrelated with each other across the population. A principal components analysis was applied to our wave-aberration measurements with the resulting principal components providing only a slightly more compact description of the population data than Zernike modes. This indicates that Zernike modes are efficient basis functions for describing the eye's wave aberration. Even though there appears to be a random variation in the eye's aberrations from subject to subject, many aberrations in the left eye were found to be significantly correlated with their counterparts in the right eye. © 2001 Optical Society of America

OCIS codes: 330.7310, 330.5370, 330.4460.

1. INTRODUCTION

Aberrations of the human eye play a major role in degrading retinal image quality.[1] From a fundamental point of view, it is necessary to have an adequate representation of the aberrations in the population to understand the nature of each particular aberration and to seek anatomical causes for individual variations. While conventional contact lenses or spectacles correct the eye's second-order aberrations (sphere and cylinder), it has been shown that higher-order aberrations have a significant impact at larger pupil diameters, further degrading the retinal image. Developing a firm understanding and compact description of the aberrations beyond defocus and astigmatism is crucial for simplifying their correction by means of customized contact lenses or laser refractive surgery.[2,3]

The most familiar approach used to quantify optical aberrations is the Seidel representation, defined for rotationally symmetric systems.[4–6] Unfortunately, the Seidel expansion is infrequently used when describing ocular aberrations, since the eye's optics are not rotationally symmetric. Taylor polynomials have also been used to describe the eye's aberrations.[7] More recently, Zernike polynomials[8] have been used to represent ocular aberrations due to their desirable mathematical properties for circular pupils.[1,9–12] They consist of an orthogonal set of polynomials that represent balanced aberrations. In addition, they are also related to the classical Seidel aberrations.[13] However, we wished to further investigate the possible existence of a more compact description of the eye's wave aberration. Such a description would exist if there were correlations between Zernike modes in the population.

Howland and Howland studied the monochromatic aberrations of 33 subjects by using the aberroscopic technique and found that the wave aberration differs greatly from subject to subject.[7] Even though Howland and Howland later improved their technique with Walsh and Charman,[14] the initial large-scale measurements were done subjectively, and their new objective measurements were made on only 11 subjects. Smirnov was one of the first investigators to begin looking at intersubject variability in the eye's wave aberration for a population of ten subjects.[15] Guirao *et al.* also documented the variability of the eye's aberrations between subjects using double-pass retinal images recorded at different pupil diameters for paralyzed accommodation.[16] From all of these previous studies, it is apparent that there is a large variation in the eye's optical quality between subjects. Applying a statistical analysis, such as principal-components analysis, to wave-aberration data measured in a large popula-

0740-3232/2001/081793-11$15.00 © 2001 Optical Society of America

tion would determine if the intersubject variations in aberration structure were purely random.

We used a Hartmann–Shack wave-front sensor that was based on the technique devised by Liang *et al.*[9] to measure the monochromatic wave aberrations of both left and right eyes in a large population of 109 normal subjects. These wave aberrations serve as a reference for the type of aberrations that are characteristic of a normal population. We also sought to determine the magnitude and variability of all aberrations in the population. This investigation could provide valuable insight on the visual benefit that could be theoretically obtained from a customized correction of the eye's monochromatic aberrations from person to person.

Finally, we investigated the differences and similarities in the pattern of the monochromatic aberrations in the human population. A principal components analysis[17] was performed on wave-aberration data to search for a more compact and efficient description of the eye's aberrations in the population. This analysis could offer a possible approach to simplifying the prescription for correcting higher-order aberrations with customized lenses or laser surgery and could also provide insight into the anatomical causes for individual wave aberrations.

2. METHODS

A. Experimental Design

Two modified Hartmann–Shack wave-front sensors were used to measure the wave aberration, one at the University of Rochester and the other at Bausch & Lomb. Figure 1 shows the two experimental systems, in which planes conjugate with the eye's pupil are labeled *p* and planes conjugate with the retina are labeled *r*. Both systems incorporated a pupil camera having an optical axis coincident with that of the wavefront sensor, which was used to center each subject's pupil while the subject looked at the center of the fixation target. An infrared superluminescent diode (SLD) emitted collimated linearly polarized light at 780 nm and had a short coherence length of approximately 30 μm. This light source reduced speckle in the Hartmann–Shack images and served as a comfortable viewing source for the subject. The total irradiance on the cornea was 6 μW, which is approximately 30 times below the American National Standards Institute maximum permissible exposure for continuous viewing at this wavelength.[18] In one system, a scanning mirror was also inserted in a plane conjugate with the pupil to further reduce speckle by averaging the noise in our images. As described and illustrated by Hofer *et al.*,[19] this mirror scanned the beam across a very small portion of the retina at a rate of 600 Hz while descanning the reflected beam on the return path through the eye's pupil. Therefore the entering beam and the reflected wave front did not move in the pupil plane of the eye.

The beam from the SLD that was focused on the retina acted as a point source, and the light emerging from the pupil formed the aberrated wave front. A focus corrector was used to reduce the defocus present in the Hartmann–Shack images by placing the retina conjugate with the SLD and the CCD camera. The aberrated wave front propagated back through the system and was reflected by

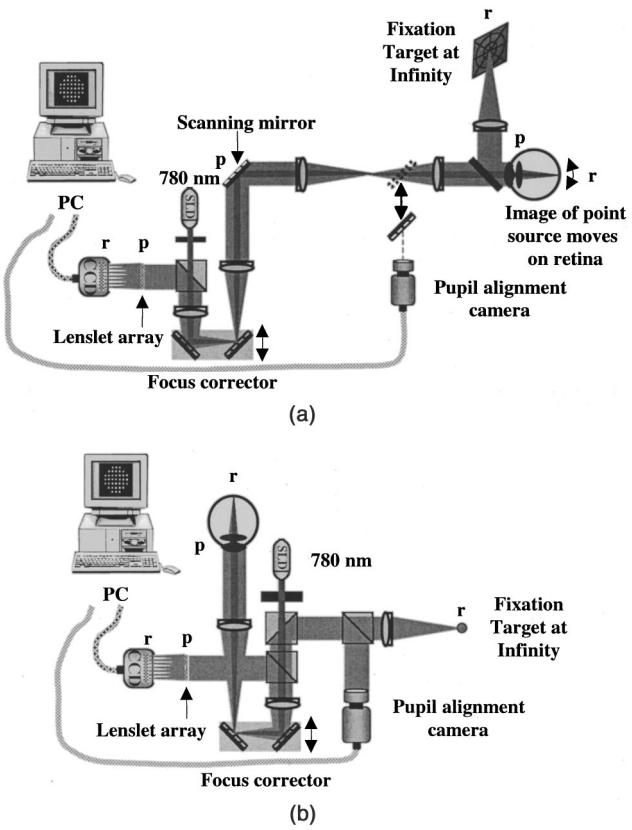

Fig. 1. Hartmann–Shack wave-front sensors used to measure the eye's aberrations at (a) the University of Rochester and (b) Bausch & Lomb. The light from the SLD serves as a beacon, forming a point source on the retina. Light reflected from the retina emerges through the eye's pupil as an aberrated wavefront and is propagated through the system to the lenslet array, placed conjugate with the eye's pupil. Each lenslet forms a focused spot on the CCD, yielding an array of spots that finely samples the pupil. The wave aberration is determined from the Hartmann–Shack image.

the polarizing beamsplitter toward the lenslet array. The polarizing beamsplitter rejected the polarized light reflected from the cornea and reflected the depolarized component from the retina. The lenslet array was placed in a plane conjugate with the eye's pupil and had an interlenslet spacing of 0.6 mm and a focal length of 40 mm. Light from each lenslet was then focused to a spot on the CCD camera placed in the back focal plane of the lenslet array. A total of 57 lenslets were used to sample a 5.7-mm pupil. The CCD camera then recorded the spot array pattern and sent the image to a PC to determine the wave aberration. Due to the eye's aberrations, each spot tended to shift from its normal diffraction-limited on-axis location on the CCD camera. On the basis of these relative spot displacements, we determined the local slope of the wave front at each lenslet. We then reconstructed the eye's wave aberration using a least-squares technique.[20]

B. Subjects

Our population consisted of 109 normal subjects, each having a spherical refraction between +6.00 D and −12.00 D and a refractive astigmatism of less than −3.00 D. No restrictions were placed on corneal curvature re-

quirements. The subjects ranged in age between 21 and 65 years and had a mean age of 41 years. The number of subjects measured in each age group is shown in Fig. 2. Subjects having any type of pathology (i.e., cataracts, keratoconus, etc.) or surgery, including laser refractive surgery, were not included in this study. Most subjects had a pupil diameter larger than 5.7 mm. For these subjects, the wave aberration over the central 5.7 mm of the pupil was used in the study. The few subjects having a natural pupil smaller than 5.7 mm were not included in our population of 109 normal subjects, since their wave aberration could not be determined for the 5.7-mm pupil size.

C. Experimental Procedure

We measured the wave aberration of left and right eyes of the 109 subjects under natural (or unparalyzed) accommodation for a 5.7-mm pupil. The subject's pupil was aligned with use of the pupil camera while the head was fixed in space with a bite-bar mount or a head-and-chin rest assembly. The subject could manually control the focus corrector and crudely adjust its position until the SLD was roughly in focus on the retina. We then fine tuned the focus corrector until the subject's sphere, as determined by the wave-front sensor, was removed. This procedure produced high-quality spots, the centroids of which were easy to compute. At least three Hartmann–Shack images, each with an exposure time of 500 ms, were collected in both eyes. Subjects maintained their fixation on the target that was placed at infinity. The wave aberration was calculated up to and including fifth order by using 18 Zernike terms (modes 4 through 21) over a 5.7-mm pupil. From these measurements, we obtained an average wave aberration for each eye.

Natural accommodation did not play a significant role in altering our measurements, since all subjects fixated on a target placed at infinity and their mean wave aberration was determined by averaging the reconstructed wave front obtained from several Hartmann–Shack images. The average of all the standard deviations for each subject over a 5.7-mm pupil was 0.11 μm (0.10 D) for defocus, indicating a stable accommodative state. We also verified that there were no systematic variations between the measurements obtained from Bausch & Lomb's wave-front sensor and those obtained by the University of Rochester wave-front sensor. The correlation coefficient of the equivalent sphere (sphere minus half of the cylinder, in diopters) measured at the two separate locations for 11 subjects across a 5.7-mm pupil was 0.98 ($p < 0.0001$), and the slope of the best fit line was 1.009. In addition to examining the degree of correlation between equivalent sphere measurements obtained from the two systems, we separately correlated the second-, third-, fourth-, and fifth-order Zernike coefficients from the average wave aberrations of both right and left eyes of the same 11 observers. The Zernike coefficients for each order were also significantly correlated ($p < 0.0001$) with high correlation coefficients. These results indicate an excellent correlation between measurements obtained on both systems for the same individuals.

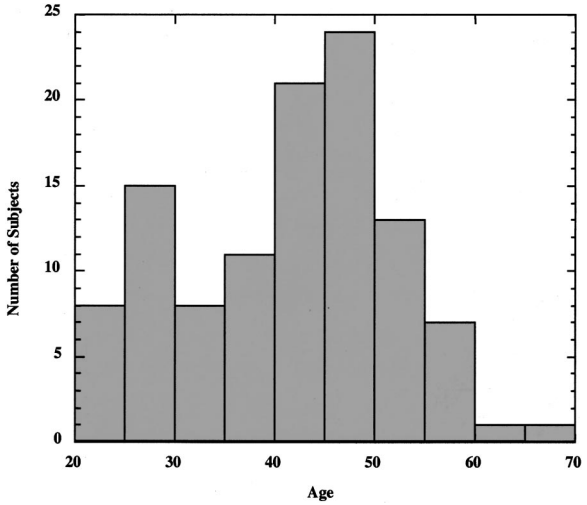

Fig. 2. Distribution of age for the 109 normal subjects included in our population study.

D. Theory of Principal Components Analysis

The purpose of performing a principal components analysis on wave aberrations is to investigate the possible existence of a more efficient set of basis functions that capture nearly all of the aberration structure in our population that is present in a conventional Zernike description. Using principal components analysis, we constructed a new set of basis functions that account for as much of the variance (i.e., dispersion) of the original data as possible with the minimum number of basis functions.[17] These new functions, or principal components, are uncorrelated across the population and are linear combinations of Zernike modes. The first principal components may be selected to retain as much of the variance of the original data as possible, providing a compact and more efficient description of the wave aberration in the population that incorporates some of the effects of higher-order aberrations. As a simple example, a principal components analysis performed on wave-aberration data containing two Zernike modes that are highly correlated with each other would express these modes more efficiently when using one principal component that is a weighted sum of the two Zernike modes.

We applied a principal-components analysis separately to the wave-aberration data of the left and right eyes of the 109 normal subjects, transforming the variables describing the wave aberration (18 Zernike coefficients) into new uncorrelated variables that are combinations of the initial variables. The wave aberration for both eyes of each subject, WA_j, was first measured and represented using a combination of 18 Zernike modes:

$$WA_j = \sum_{i=1}^{18} A_{ij} Z_i, \tag{1}$$

where A_{ij} are the Zernike coefficients corresponding to their particular Zernike mode, Z_i, for subject j. The variance for each Zernike coefficient across the population was then calculated, and the wave aberration was rearranged for all subjects so that the Zernike modes were ordered from the Zernike coefficient with the highest variance to that with the lowest. This technique allows the Zernike representation to become as efficient as possible.

We then constructed two 109×18 matrices, one for each eye, with the Zernike coefficients as the variables in columns and each subject's average wave aberration in rows. An example of one of these matrices, **X**, is shown in Eq. (2):

$$\mathbf{X} = \begin{array}{l} \\ \text{Subject 1} \\ \text{Subject 2} \\ \vdots \\ \text{Subject 109} \end{array} \begin{array}{ccccc} Z_2^{\,0} & Z_2^{\,2} & Z_2^{\,-2} & \cdots & Z_5^{\,-3} \\ A_{1,1} & A_{2,1} & A_{3,1} & \cdots & A_{18,1} \\ A_{1,2} & A_{2,2} & A_{3,2} & \cdots & A_{18,2} \\ \cdots & \cdots & \cdots & \cdots & \cdots \\ A_{1,109} & A_{2,109} & A_{3,109} & \cdots & A_{18,109} \end{array}. \tag{2}$$

From the matrix **X** we calculated the covariance matrix **C**

$$\mathbf{C} = \mathrm{Cov}(A_{ij}). \tag{3}$$

In this covariance matrix, the off-diagonal elements indicate the degree of correlation between two particular Zernike coefficients. This correlation increases as the element's value increases, with zero values indicating no correlation between a pair of Zernike modes. We then calculated the eigenstructure of matrix **C** to find the new, uncorrelated variables. Diagonalizing matrix **C** by means of

$$|\mathbf{C} - \lambda \cdot \mathbf{I}| = 0 \tag{4}$$

$$(\mathbf{C} - \lambda \cdot \mathbf{I}) \cdot \vec{\mathbf{v}} = 0, \tag{5}$$

where **I** is the identity matrix, we obtained the eigenvalues (λ) and eigenvectors ($\vec{\mathbf{v}}$). We can combine each eigenvector into a single matrix **V** having the eigenvectors ($\vec{\mathbf{v}}$) in columns. **V** then transforms the original Zernike base into the new basis functions, or principal components, or

$$\widetilde{\mathbf{PC}} = \mathbf{V} \cdot \vec{\mathbf{Z}}. \tag{6}$$

The wave aberration may now be expressed as a new expansion by using the new principal components as

$$WA_j = \sum_{i=1}^{18} A_{ij}' PC_i, \tag{7}$$

and A_{ij}' are the coefficients of the new principal components, PC_i.

3. RESULTS

A. Distribution of the Eye's Aberrations

The average absolute rms wave-front error of each Zernike mode and their relative contributions to the entire wave aberration are shown in Fig. 3(a) from both eyes of our population. The double-indexing scheme used to label the Zernike coefficients corresponds with the standard labeling notation established by the Vision Science and Its Applications Standards Taskforce team.[21] As seen in the figure, Zernike defocus ($Z_2^{\,0}$) accounts for 80% of the total variance of the wave aberration and has the largest magnitude of any mode (mean absolute rms of 3.39 μm or 2.89 D). The magnitude of this defocus coefficient is larger than that for a purely randomly selected, normal population due to the fact that most of our population consisted of patients from a clinic at Bausch & Lomb who tended to be myopic. According to the most recent large-scale measurements of the refractive errors performed on randomly sampled patients in the United States, approximately 25% of the population between the ages of 12 and 54 years are myopic.[22] Our study contained more than twice the percentage of myopic subjects when compared with the population-based data, as nearly 60% of our subjects were myopic.

The next largest contributors to the wave aberration in the population are the astigmatic modes, $Z_2^{\,2}$ and $Z_2^{\,-2}$, with the first three modes accounting for over 92% of the total variance of the wave aberration. Figure 3(b) shows the dispersion of each Zernike mode in the population.

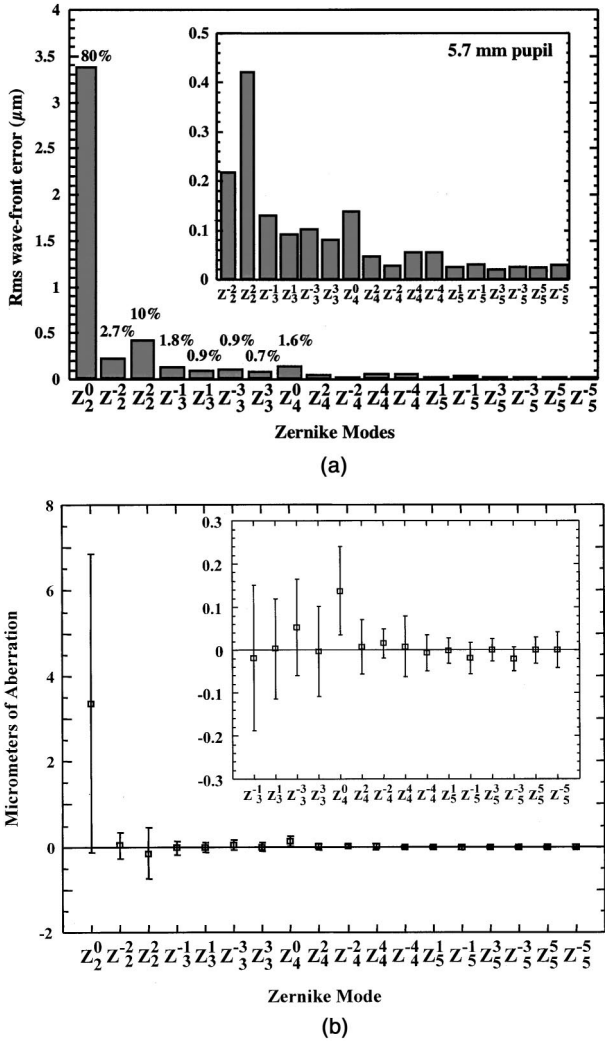

Fig. 3. (a) Mean absolute rms wave-front error of all 18 Zernike modes for the 109 normal subjects across a 5.7-mm pupil. The percentages listed above the first eight modes represent the percentage of the variance of the wave aberration accounted for by each Zernike mode. The magnitudes of the higher-order aberrations may be seen in the inset figure, which shows all modes except Zernike defocus ($Z_2^{\,0}$) with the ordinate expanded. (b) Mean values of all Zernike modes in the population across a 5.7-mm pupil. The error bars represent plus and minus one standard deviation from the mean value. The variability of the higher-order modes is shown in the inset of the figure, which excludes all second-order modes ($Z_2^{\,-2}$, $Z_2^{\,0}$, and $Z_2^{\,2}$) and again expands the ordinate.

Table 1. Correlation Coefficients for Each Zernike Mode between the Left and Right Eyes of All 109 Subjects and the Modes That are Significantly Correlated

Zernike Coefficient	Correlation Coefficient	Significantly Correlated $P < 0.01$
Z_2^{-2}	−0.4788	Yes
Z_2^{0}	0.9772	Yes
Z_2^{2}	0.7724	Yes
Z_3^{-3}	0.5365	Yes
Z_3^{-1}	0.6856	Yes
Z_3^{1}	−0.4345	Yes
Z_3^{3}	−0.3558	Yes
Z_4^{-4}	−0.0963	No
Z_4^{-2}	−0.1551	No
Z_4^{0}	0.8219	Yes
Z_4^{2}	0.5388	Yes
Z_4^{4}	0.5554	Yes
Z_5^{-5}	0.2942	Yes
Z_5^{-3}	0.4258	Yes
Z_5^{-1}	0.4331	Yes
Z_5^{1}	0.0802	No
Z_5^{3}	−0.0415	No
Z_5^{5}	0.0805	No

The means of almost all Zernike modes, except for spherical aberration, are approximately zero and have a large intersubject variability. Spherical aberration has a mean value (± one standard deviation) of $+0.138 \pm 0.103\ \mu$m and is the only mode to have a mean that is significantly different from zero. The magnitudes of the higher-order aberrations generally decline with order, except for spherical aberration, which is larger in mean absolute rms than any third-order mode.

B. Correlations between Left and Right Eyes

Table 1 shows correlation coefficients for each Zernike mode between left and right eyes in the population. (This statistical correlation test was performed on each Zernike mode individually, and no correction was applied for multiple tests.) Zernike defocus (Z_2^0) had the highest correlation coefficient (0.9772) between both eyes. Primary spherical aberration (Z_4^0) had the next highest value (0.8219), followed by that for astigmatism, Z_2^2 (0.7724). Table 1 also shows which modes in the left eye are significantly correlated with their counterparts in the right eye for a confidence level of $p < 0.01$. Nearly 75% of the Zernike modes are significantly correlated across eyes (13 out of 18 modes) for $p < 0.01$. In addition,

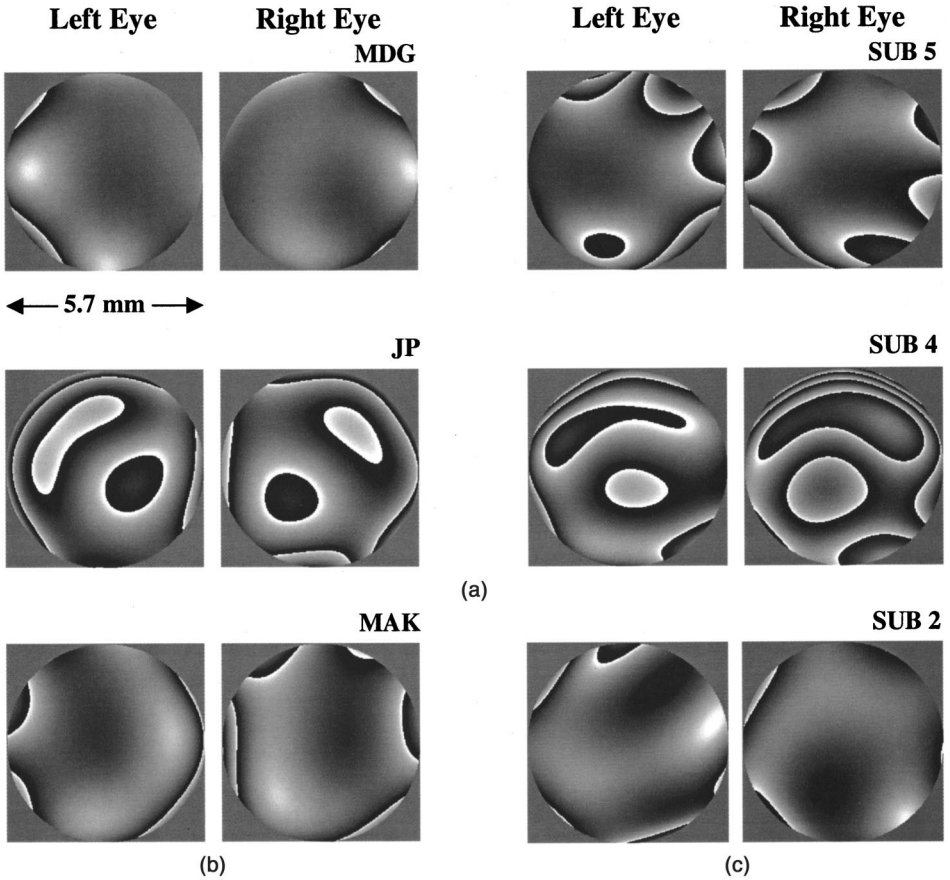

Fig. 4. Mirror symmetry in the wave aberration between left and right eyes for a 5.7-mm pupil. Defocus and astigmatism (second-order modes Z_2^{-2}, Z_2^0, and Z_2^2) were not included in the wave aberration. (a) Plots of the wave aberration of left and right eyes of four subjects that show a high degree of mirror symmetry between eyes. (b) Plots of the wave aberration of both eyes for subject MAK, who shows a lesser degree of symmetry across eyes. Not all subjects display the near-perfect mirror symmetry between left and right eyes as evidenced in (a). (c) An example of one of the few subjects who displays almost no mirror symmetry in the wave aberration between left and right eyes.

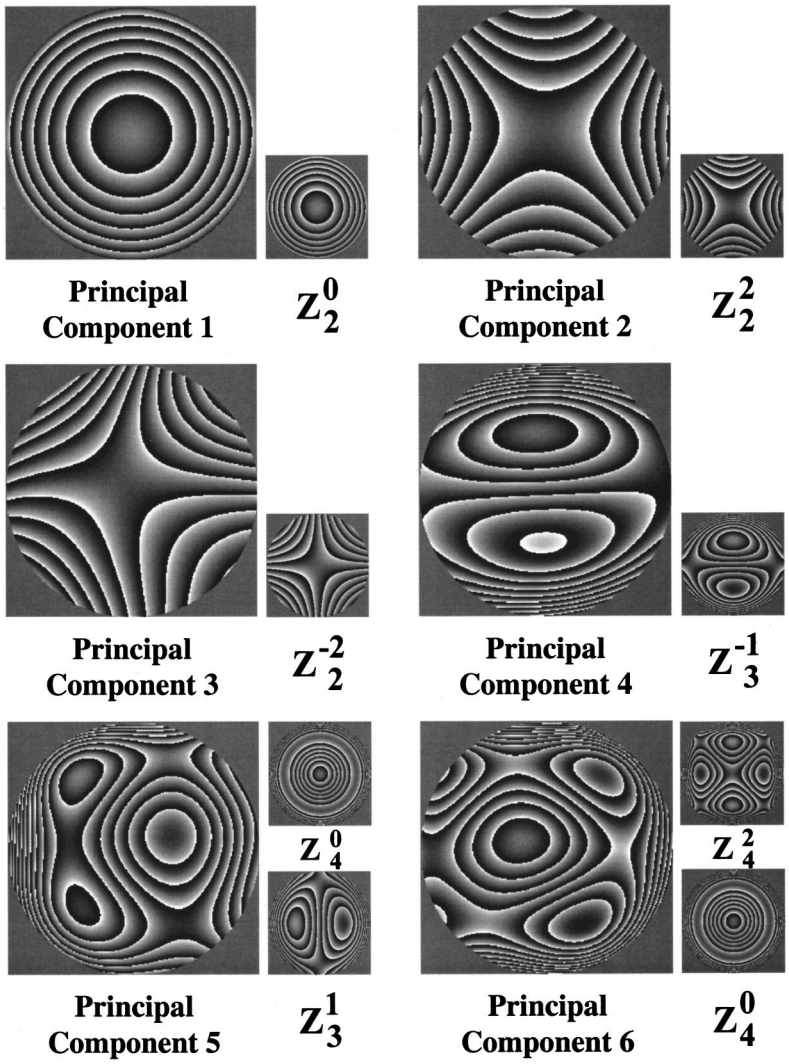

Fig. 5. The first six principal components used to describe the wave aberration of the normal population. Adjacent to each principal component is a picture of the Zernike mode that is most highly correlated with that particular principal component. The first few principal components are very similar to lower-order Zernike modes.

over half of all Zernike modes (61%) in the left eye are significantly correlated with those in the right for $p < 0.001$.

This high degree of correlation between Zernike modes in left and right eyes suggests that some form of symmetry exists between the wave aberrations of each eye within an individual and is in agreement with results reported by Liang and Williams.[1] This mirror symmetry between left and right eyes can be seen in Fig. 4(a), which shows the wave aberrations of both eyes for four subjects across a 5.7-mm pupil. Even though several subjects have similar aberrations between left and right eyes, some subjects have only a moderate amount of symmetry in their eye's wave aberrations [as in Fig. 4(b)], while a few show almost no symmetry [as in Fig. 4(c)]. To address the prevalence of mirror symmetry in our population, for each subject we plotted the coefficients of individual Zernike modes (excluding defocus and astigmatism) in the right eye against their corresponding value in the left eye and determined their associated correlation coefficient. The signs of all appropriate Zernike coefficients that exhibited odd symmetry about the y axis were flipped in one eye and not the other. The mean correlation coefficient ($\pm$ one standard deviation) for all 109 individuals was 0.5717 ± 0.2497, indicating that most subjects had a fair amount of mirror symmetry in the wave aberration between both eyes.

Evidence of mirror symmetry between left and right eyes is also illustrated in Table 1, which shows correlation coefficients with both positive and negative values. A positive correlation coefficient indicates that Zernike coefficients in one eye of the population are increasing in the same direction as their counterparts in the other eye. A negative correlation coefficient implies that the Zernike values in one eye are increasing as their counterparts in the other eye are decreasing in value. To have perfect mirror symmetry between right and left eyes, radially symmetric Zernike modes and those dependent on an odd power of y need to be positively correlated in both eyes, while polynomials that are dependent on an odd power of x should be negatively correlated in both eyes. For example, a Zernike mode dependent on an odd power of x would possess mirror symmetry if it increased in value (more positive) for the left eye while simultaneously de-

creasing in value (more negative) for the right eye. To have perfect mirror symmetry, we would expect to obtain negative correlation values for Zernike modes Z_2^{-2}, Z_3^{1}, Z_3^{3}, Z_4^{-2}, Z_4^{-4}, Z_5^{1}, Z_5^{3}, and Z_5^{5}. From Table 1, we see that all eight of these modes are negatively correlated in left and right eyes, except for Z_5^{1} and Z_5^{5}. However, these two modes have very small correlation coefficients and are not significantly correlated in both eyes even when we reduce the confidence level to $p < 0.05$. All of the remaining ten modes that are either radially symmetric or depend on an odd power of y have positive correlation coefficients (as expected for mirror symmetry).

C. Principal Components Analysis

The first six principal components obtained from the wave-aberration measurements of the left eye are shown in Fig. 5. The Zernike mode that is most highly correlated with each principal component is illustrated next to all of the principal components. We obtained similar results for the right eye. The first four principal components nicely map onto the first four Zernike modes. Principal component 1 is strongly correlated with defocus (Z_2^{0}), while principal component 2 is most highly correlated with astigmatism (Z_2^{2}). The effects of higher-order aberrations captured by the first few principal components begin to become visible in the third principal component, most highly correlated with diagonal astigmatism (Z_2^{-2}). Principal component 4 is significantly correlated with vertical coma (Z_3^{-1}) and vertical triangular astigmatism (Z_3^{-3}). Principal components 5 and 6 are both significantly correlated with horizontal coma (Z_3^{1}), spherical aberration (Z_4^{0}), and Z_4^{4}. However, principal component 5 also consists of a significant amount of horizontal triangular astigmatism (Z_3^{3}), while principal component 6 is highly correlated, instead, with secondary astigmatism (Z_4^{2}) and Z_5^{5}.

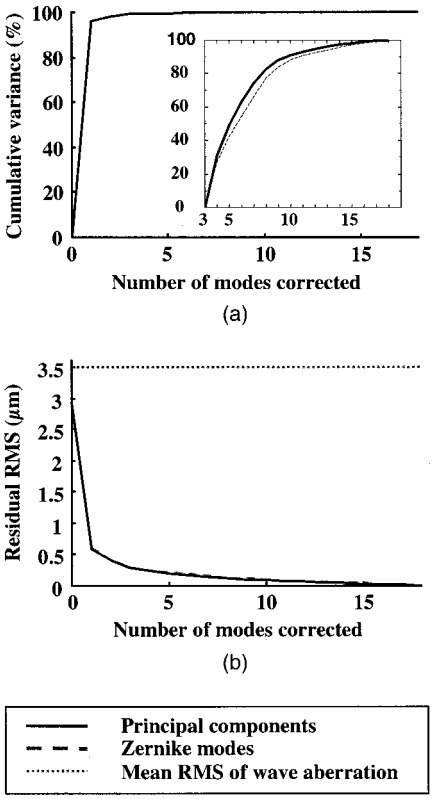

Fig. 6. Similarity between a principal component and Zernike representation of the wave aberration in the population for left eyes only (5.7-mm pupil). The solid curves show a principal components description of the wave aberration, and the Zernike representation is illustrated by a dashed curve. The Zernike modes were ordered from the Zernike coefficient having the highest variance to that with the lowest. (a) Percentage that each mode contributes to the cumulative variance across the population. Zernike defocus and principal component 1 account for over 90% of the cumulative variance. The inset figure shows the cumulative contribution of higher-order modes on the residual variance upon removing the contributions from the first three Zernike modes (defocus and astigmatism) and the first three principal components. The percent of the contribution has been renormalized so that modes 1–3 have no contribution to the cumulative residual variance and modes 4–18 have a contribution of 100%. (b) The mean rms wave-front error (in micrometers) of the residual wave aberration when a given number of Zernike modes or principal components are corrected in the wave aberration of our population. The dotted line shows the mean rms of the wave aberration when no modes are corrected for all normal subjects. Both descriptions yield nearly identical results.

As shown in the following figures, a principal components representation of the wave aberration in the population provided a modest improvement over a conventional Zernike description, with both eyes producing nearly the same results. The percentage that each mode contributes to the cumulative variance (i.e., dispersion) for the left eyes of the population is shown in Fig. 6(a). In addition, the average rms of the residual wave aberration in our population as more modes are corrected over a 5.7-mm pupil is shown in Fig. 6(b). Defocus alone accounts for over 90% of the cumulative variance in the population and, on average, increases the mean rms of the residual wave aberration by over 2 μm. The subject selection criteria, which allowed our population to have a broad range of spherical refractive powers, explains the overwhelming contribution of the defocus term when compared with the other aberrations.

With the exception of some slight deviations between the two curves, Fig. 6 appears to indicate that a Zernike description of the wave aberration in the population is nearly as efficient as a principal components description. Even when we remove the contributions from the first three Zernike modes and principal components, the inset in Fig. 6(a) shows only a small difference in the contribution of higher-order modes to the residual variance between a principal components and Zernike description of the wave aberration. To investigate whether these slight deviations were important for retinal image quality, we evaluated each subject's Strehl ratio after correcting a particular number of Zernike modes or principal components. The average results from the analyses on both eyes for each subject with use of both descriptions are shown in Fig. 7. The subjects lying within the ellipse in Fig. 7(b) are outliers in the population who have larger amounts of higher-order aberrations (i.e., lower residual Strehl ratios) compared with most subjects when using a Zernike description of the wave aberration. However, when these same subjects have their wave aberration expressed with principal components, they now obtain residual Strehl ratios that are similar to the rest of the population. Figure 7 illustrates the concept that principal components more effectively describe the wave aber-

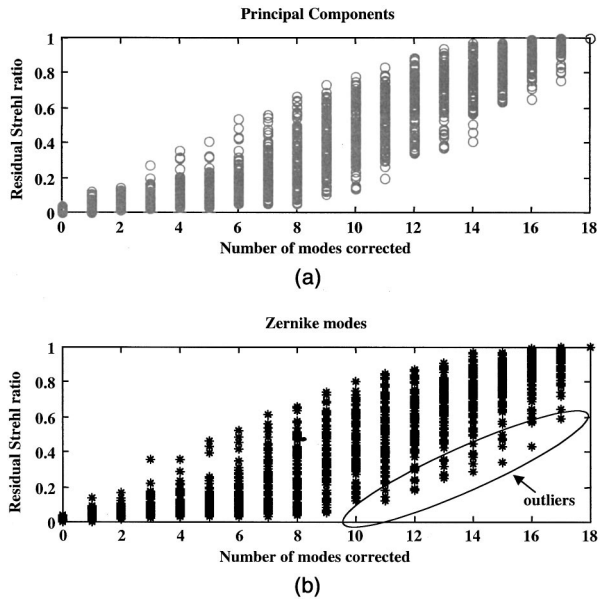

Fig. 7. Dispersion of the residual Strehl ratio for each subject (averaged from the separate analyses performed on left and right eyes) when a fixed number of (a) principal components or (b) Zernike modes are corrected in the wave aberration (5.7-mm pupil).

ration of subjects in the population who have large amounts of higher-order aberrations.

By averaging each subject's residual Strehl ratio when correcting a given number of modes, we were able to obtain two curves showing the mean Strehl ratio for both a Zernike and principal component description of the wave aberration. Figure 8 shows the mean residual Strehl ratios for our population based on the results shown in Fig. 7. If a fixed number of modes were corrected in the eye, the average image quality would be slightly higher with principal components than with Zernike modes. In addition, depending on the number of modes corrected, one can obtain the same average image quality in the eye by using one less principal component than Zernike mode or nearly the same number of principal components and Zernike modes. For example, a conventional correction of the first three Zernike modes (defocus and two astigmatism terms) yields the same average residual Strehl ratio (0.075) as an equivalent correction of the first three principal components. Both descriptions for an uncorrected eye also produce identical average residual Strehl ratios of 0.01.

Figure 9 illustrates the similar effects of using principal components or Zernike modes to describe the eye's wave aberration. When correcting a fixed number of modes in the eye, this figure compares the percentage of subjects who could achieve a Strehl ratio greater than 0.1, 0.3, or 0.8 with principal components or Zernike modes. The results obtained from the separate analyses of the left and right eyes were averaged in order to produce each of the six curves shown in the figure. Again, we see that it is slightly more efficient to express the wave aberration using principal components. 73% of normal subjects could achieve a Strehl ratio greater than 0.1 by correcting six principal components, whereas only 55% would achieve this value when correcting six Zernike modes. The results for the two curves with subjects having Strehl ratios larger than 0.3 are nearly identical, with the largest discrepancies occurring when 11 or 12 modes are corrected. Correcting 16 principal components or 17 Zernike modes allows over 91% of the subjects to obtain a Strehl ratio greater than 0.8. This last observation is to be expected, since our wave-aberration measurements only included 18 Zernike modes. Therefore correcting all 18 modes would yield a perfect Strehl ratio of 1 for every subject.

4. DISCUSSION

As shown in Table 1, we were able to track the correlation in aberration structure between left and right eyes for the same observer. In agreement with previous reports, there is a tremendous variability in the eye's aberrations from person to person.[1,7,14] However, within an individual observer, there are several aberrations that are significantly correlated across both eyes other than conventional defocus and astigmatism. As earlier suggested by Liang and Williams,[1] we find that there is a systematic structure in the eye, with 75% of the measured Zernike modes in the left eye being significantly correlated with their counterparts in the right. This mirror symmetry in the wave aberration between left and right eyes was illustrated in Fig. 4.

This tendency for the eye's aberrations to be symmetric between left and right eyes could be explained by genetic and anatomical factors. Just as the shape of one side of the human body generally mimics the other (with some subtle variations), the aberrations in the left eye are generally mirror symmetric with those in the right with some small differences. Wyatt found that the shape of the eye's pupil tended to be mirror symmetric between left and right eyes of the same observer.[23] The fact that facial features present on each half of the same face generally possess the same structure could influence this tendency toward symmetry. It is also interesting to note that Rynders *et al.* found a significant positive correlation in the vertical shift of the pupil location from the visual axis between left and right eyes of the same individual but not in the horizontal meridian for their population.[24] Thus one would expect a strong correlation between aberrations in both eyes, such as vertical coma, that are induced by a vertical displacement of the pupil, but not for horizontal coma. As illustrated in Table 1, we found that both horizontal coma and vertical coma were significantly correlated between left and right eyes for our population. Therefore the amount of coma observed in the wave aberrations of our subjects is not simply caused by a decentration of the eye's pupil.

Even though several aberrations are correlated across eyes, there appears to be a random variation in the eye's aberrations from subject to subject, since most Zernike modes are uncorrelated with each other across the population. These correlation results between Zernike modes across the population were already illustrated in Fig. 5, as the first few principal components were significantly correlated with only one or two lower-order Zernike modes. We see that the aberrations inherent in the eye's optics across subjects are analogous to the variation dis-

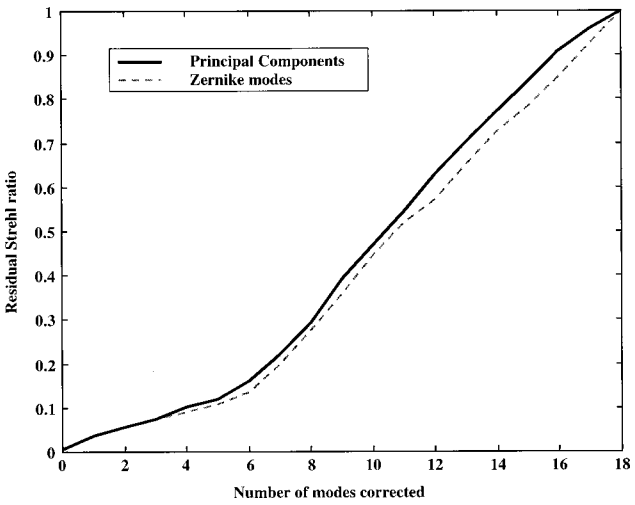

Fig. 8. The mean residual Strehl ratio (based on Fig. 7) for all normal subjects when correcting a fixed number of principal components (solid curve) or Zernike modes (dashed curve) across a 5.7-mm pupil. Principal components are slightly more efficient and yield slightly better image quality than Zernike modes. Correcting one fewer or the same number of Zernike modes as principal components can provide the same average image quality in the eye.

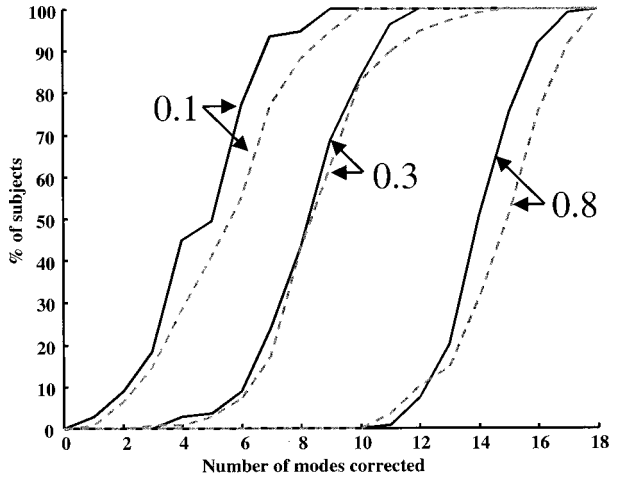

Fig. 9. Percentage of subjects having a residual Strehl ratio greater than 0.1, 0.3, or 0.8 when correcting a given number of principal components (solid curves) or Zernike modes (dashed curves) for a 5.7-mm pupil. (Each curve was obtained by averaging the results obtained from the separate analyses of the left and right eyes.) For all three values of the Strehl ratio, principal components provide a more efficient representation of the eye's wave aberration in the population.

played when we look at different sets of fingerprints. Just as the eye's optics are generally mirror symmetric in the left and right eyes of the same person (Fig. 4), fingerprints on the left hand are often very similar with those on the right hand within the same individual.[25] However, the spatial arrangement and patterns of finger ridges can vary dramatically from person to person.[26]

It would be valuable to also investigate anatomical mechanisms that could be responsible for the lack of significant correlation between aberrations we observe across the population. In particular, there was no significant correlation between defocus and astigmatism or defocus and spherical aberration. A strong correlation between defocus and spherical aberration might not be expected, since these two aberrations result from different anatomical factors. The amount of defocus an individual possesses is highly dependent on the axial length of the eye,[27] whereas the amount of spherical aberration inherent in an individual's wave aberration strongly depends on the patient's corneal curvature and the shape of the crystalline lens.[28,29] Therefore a change in the subject's value of defocus would suggest a change in the axial length of the eye and not necessarily in the corneal or lens shape or spherical aberration value. This, in fact, is what we observed for our subject pool, as we found that defocus and spherical aberration were not significantly correlated across the population.

Some other anatomical mechanisms that might produce correlations in aberration structure could be a decentration of the pupil or the misalignment of different optical surfaces (cornea, pupil, and lens) in the eye. These elementary mechanisms, however, would likely produce some correlated aberrations across the population. A simple case in which one would expect the presence of a strong correlation between two Zernike modes might occur for a displacement of the eye's pupil across the population. A decentration of the pupil would typically produce, among other aberrations, significant amounts of coma and secondary coma. These two aberrations would be strongly correlated across the population and would therefore be expressed as a single basis function in a principal components analysis. We did not find a significant correlation between coma and secondary coma in our population, though, and believe that this anatomical mechanism cannot explain some of the variability exhibited in aberration structure in our population. In general, it seems that a more sophisticated mechanism must be responsible for producing individual aberrations such as coma and secondary coma in the eye's wave aberration. In addition, several anatomical mechanisms could all be responsible for generating the entire structure of the wave aberration in most eyes, with different mechanisms acting as the dominant sources of aberrations in different groups of eyes.

One of the main reasons for performing a linear (or principal components) analysis on the population data was to find the most robust set of basis functions that would completely and adequately describe the wave aberration of the human eye across the population. The resulting principal components retain as much of the variance of the original Zernike modes as possible and can also serve to extract strong correlations between Zernike modes. It is possible that a different type of analysis, such as a nonlinear analysis, could reveal correlations between Zernike modes that were not captured using a linear principal components description. For example, if a quadratic correlation existed between the Zernike defocus and astigmatism modes, principal-components analysis would fail to adequately capture this correlation, since it is a linear technique. A nonlinear analysis, on the other hand, could best describe this pattern in aberration structure. Nevertheless, we believe that we would have found at least some small correlation between Zernike modes using a principal components analysis if this were the

case, with the correlated Zernike modes being incorporated into individual principal components. Our results show that there is almost no correlation between Zernike modes when we look across the population.

Our principal components analysis was performed on 109 normal subjects whose refractive errors were different and widely distributed over a broad range. Principal components analysis extracts strong correlations between Zernike modes across this population but does not preclude the fact that some individuals in the population could have similar clusters of aberrations that are weakly and structurally correlated. If a particular spatial pattern in the wave aberration existed within different refractive groups, performing this analysis across all refractive groups could have masked any special structure inherent in these groups. For example, if defocus was positively correlated with certain higher-order aberrations in myopic eyes, but was negatively correlated with these same aberrations in hyperopic eyes, a principal components analysis would find almost no correlation between defocus and the higher-order aberrations. The positive and negative correlations would tend to cancel each other with this analysis, resulting in the detection of no correlations between these aberrations. This is due to the fact that principal components analysis examines correlations across the entire population of eyes.

Therefore, to help explore the possibility that some small group of individuals within the population had a similar pattern of aberrations, we examined the degree of correlation between Zernike modes within three different refractive groups: myopic subjects with a spherical refraction between -12 D and -1 D, emmetropic subjects having a spherical refraction between -1 D and $+1$ D, and hyperopic subjects with a spherical refraction from $+1$ D to $+6$ D. We found no difference in the number of significant correlations between Zernike modes when comparing these three groups with the entire population. We also found no correlation between the rms value of the eye's higher-order aberrations and each subject's refraction, implying that there is no link between myopia and higher-order aberrations across our population. This analysis, however, does not eliminate the possibility that there may be clusters of individuals who have similar combinations of correlated aberrations other than defocus and higher-order aberrations.

Finally, as seen from Fig. 8, removing defocus and astigmatism (modes 1 through 3) from each subject's wave aberration would not have significantly altered the principal components analysis, since the same mean residual Strehl ratios were obtained when correcting the first three principal components or Zernike modes. A large separation between the two curves shown in this figure for modes 4 through 18 would have indicated that principal components were much more efficient than Zernike modes, implying the presence of correlations between individual Zernike terms. However, due to the similarity between these two curves, we again conclude that Zernike modes are relatively uncorrelated with other modes in the population. For this reason, principal components provide only a slightly more efficient description of our population data than Zernike modes. In addition to their desirable mathematical properties, Zernike polynomials are efficient basis functions for describing the wave aberration of the eye.

ACKNOWLEDGMENTS

This research was supported by National Institutes of Health grants EY01319 and EY07125 and by a grant from Bausch & Lomb. This work has also been supported in part by the National Science Foundation Science and Technology Center for Adaptive Optics (Grant 5-24182), managed by the University of California at Santa Cruz under cooperative agreement No. AST-9876783. A. Guirao thanks a fellowship from the Ministerio de Educación y Culture (Spain). The authors thank Rick J. Potvin and Michele A. Lagana for their clinical assistance in conducting subjective refractions and obtaining some wave-aberration measurements.

Corresponding author J. Porter can be reached at the address on the title page or by email at jporter@optics.rochester.edu.

*Present address, Laboratorio de Optica, Universidad de Murcia, Campus de Espinardo, 30071 Murcia, Spain.

REFERENCES

1. J. Liang and D. R. Williams, "Aberrations and retinal image quality of the normal human eye," J. Opt. Soc. Am. A **14**, 2873–2883 (1997).
2. J. Liang, D. R. Williams, and D. T. Miller, "Supernormal vision and high-resolution retinal imaging through adaptive optics," J. Opt. Soc. Am. A **14**, 2884–2892 (1997).
3. D. T. Miller, "Retinal imaging and vision at the frontiers of adaptive optics," Phys. Today **53**, 31–36 (2000).
4. W. T. Welford, *Aberrations of Optical Systems* (Hilger, Bristol, UK, 1986).
5. W. J. Smith, *Modern Optical Engineering: The Design of Optical Systems* (McGraw-Hill, New York, 1990).
6. J. C. Wyant and K. Creath, "Basic wavefront aberration theory for optical metrology," in *Applied Optics and Optical Engineering,* R. R. Shannon and J. C. Wyant, eds. (Academic, New York, 1992), Vol. XI, pp. 1–53.
7. H. C. Howland and B. Howland, "A subjective method for the measurement of monochromatic aberrations of the eye," J. Opt. Soc. Am. **67**, 1508–1518 (1977).
8. R. J. Noll, "Zernike polynomials and atmospheric turbulence," J. Opt. Soc. Am. **66**, 207–211 (1976).
9. J. Liang, B. Grimm, S. Goelz, and J. F. Bille, "Objective measurement of the wave aberrations of the human eye with the use of a Hartmann–Shack wave-front sensor," J. Opt. Soc. Am. A **11**, 1949–1957 (1994).
10. J. C. He, S. Marcos, R. H. Webb, and S. A. Burns, "Measurement of the wave front of the eye by a fast psychophysical procedure," J. Opt. Soc. Am. A **15**, 2449–2456 (1998).
11. I. Iglesias, E. Berrio, and P. Artal, "Estimates of the ocular wave aberration from pairs of double-pass retinal images," J. Opt. Soc. Am. A **15**, 2466–2476 (1998).
12. J. Schwiegerling and J. E. Greivenkamp, "Using corneal height maps and polynomial decomposition to determine corneal aberrations," Optom. Vision Sci. **74**, 906–915 (1997).
13. M. Born and E. Wolf, *Principles of Optics* (Pergamon, Oxford, UK, 1985).
14. G. Walsh, W. N. Charman, and H. C. Howland, "Objective technique for the determination of monochromatic aberrations of the human eye," J. Opt. Soc. Am. A **1**, 987–992 (1984).
15. M. S. Smirnov, "Measurement of the wave aberration of the human eye," Biophys. J. **7**, 766–795 (1962).

16. A. Guirao, C. Gonzalez, M. Redondo, E. Geraghty, S. Norrby, and P. Artal, "Average optical performance of the human eye as a function of age in a normal population," Invest. Ophthalmol. Visual Sci. **40**, 203–213 (1999).
17. I. T. Joliffe, *Principal Components Analysis* (Springer–Verlag, New York, 1986).
18. American National Standard for the Safe Use of Lasers ANSI Z136.1 (Laser Institute of America, Orlando, Fla., 1993).
19. H. Hofer, P. Artal, B. Singer, J. L. Aragon, and D. R. Williams, "Dynamics of the eye's wave aberration," J. Opt. Soc. Am. A **18**, 497–506 (2001).
20. W. H. Southwell, "Wave-front estimation from wave-front slope measurements," J. Opt. Soc. Am. **70**, 998–1006 (1980).
21. L. N. Thibos, R. A. Applegate, J. T. Schwiegerling, R. Webb and VSIA Standards Taskforce Members, "Standards for reporting the optical aberrations of eyes," in *Vision Science and Its Applications*, V. Lakshminarayanan, ed., Vol. 35 of OSA Trends in Optics and Photonics Series (Optical Society of America, Washington, D.C., 2000), pp. 232–244.
22. R. D. Sperduto, D. Seigel, J. Roberts, and M. Rowland, "Prevalence of myopia in the United States," Arch. Ophthalmol. (Chicago) **101**, 405–407 (1983).
23. H. J. Wyatt, "The form of the human pupil," Vision Res. **35**, 2021–2036 (1995).
24. M. Rynders, B. Lidkea, W. Chisholm, and L. N. Thibos, "Statistical distribution of foveal transverse chromatic aberration, pupil centration, and angle ψ in a population of young adult eyes," J. Opt. Soc. Am. A **12**, 2348–2357 (1995).
25. C. T. Naugler and M. D. Ludman, "A case-control study of fluctuating dermatoglyphic asymmetry as a risk marker for developmental delay," Am. J. Med. Genet. **26**, 11–14 (1996).
26. H. Cummins and C. Midlo, *Finger Prints, Palms and Soles: An Introduction to Dermatoglyphics* (Blakiston, Philadelphia, 1943).
27. J. P. Carroll, "Component and correlation ametropia," Am. J. Optom. Physiol. Opt. **59**, 28–33 (1982).
28. R. Navarro, J. Santamaría, and J. Bescós, "Accommodation-dependent model of the human eye with aspherics," J. Opt. Soc. Am. A **2**, 1273–1281 (1985).
29. S. G. El Hage and F. Berny, "Contribution of the crystalline lens to the spherical aberration of the eye," J. Opt. Soc. Am. **63**, 205–211 (1973).